Astron. Astrophys. 347, 47–54 (1999)

ASTRONOMY AND ASTROPHYSICS

Identification of soft high galactic latitude RASS X-ray sources

II. Sources with PSPC count rate CR < 0.5 cts/s*

K. Beuermann[1,3], **H.-C. Thomas**[2], **K. Reinsch**[1], **A.D. Schwope**[4], **J. Trümper**[3], **and W. Voges**[3]

[1] Universitäts-Sternwarte, Geismarlandstrasse 11, D-37083 Göttingen, Germany
[2] MPI für Astrophysik, Karl-Schwarzschild-Strasse 1, D-85740 Garching, Germany
[3] MPI für Extraterrestrische Physik, Giessenbachstrasse 1, D-85740 Garching, Germany
[4] Astrophysikalisches Institut Potsdam, An der Sternwarte 16, D-14482 Potsdam, Germany

Received 4 January 1999 / Accepted 4 May 1999

Abstract. We present a summary of spectroscopic identifications of bright soft high galactic latitude X-ray sources from the ROSAT All-Sky Survey with total PSPC count rates $0.11 < CR < 0.5\,\mathrm{cts\,s^{-1}}$ and hardness ratios HR1 < 0. This study supplements the identification program of a complete sample of sources with $CR \geq 0.5\,\mathrm{cts\,s^{-1}}$ presented previously. Spectroscopic identifications are presented for 70 of 77 sources, 5 sources are identified by other means, and subsidiary information is given for 2 as yet unidentified sources. In practically all cases, a unique optical counterpart exists. As for the brighter fraction of the sample, the largest source classes are Seyfert 1 galaxies, magnetic cataclysmic variables, and hot white dwarfs. In the Galactic Pole caps at $|b| \gtrsim 40°$, Seyfert galaxies dominate, whereas at intermediate latitudes galactic objects as magnetic cataclysmic variables and white dwarfs become relatively more frequent.

Key words: stars: novae, cataclysmic variables – galaxies: active – galaxies: nuclei – galaxies: quasars: general – galaxies: Seyfert – X-rays: general

1. Introduction

In Paper I (Thomas et al. 1998), we considered the complete sample of the brightest high-galactic-latitude soft X-ray sources from the ROSAT All-Sky Survey (RASS) (Voges et al. 1996, Voges 1997). For these soft sources, ROSAT is about a factor of 100 more sensitive than the HEAO-1 All-Sky Survey with the LED of the A-2 experiment (Nugent et al. 1983), suggesting a high discovery potential. Our principal aim is to determine the nature of the brightest soft X-ray sources in the RASS and perform follow-up studies of interesting individuals.

A substantial fraction of even the brightest RASS sources has optical counterparts of unknown nature (of which some are catalogued, but practically unknown). In Paper I, we demonstrated that the most frequent counterparts of the brighter previously unknown soft RASS X-ray sources are AGN, i.e. Sy1 galaxies, quasars, and BL Lac objects (66 of 126), followed by white dwarfs (WDs) together with nuclei of planetary nebulae (PNN) and PG1159 stars (25), and magnetic cataclysmic variables (14). In addition, supersoft X-ray binaries, although small in number (5), were established by ROSAT as an important class of mass-exchange systems containing what seems to be an accreting and hydrogen burning WD (e.g. Hasinger 1994, van Teeseling 1997). It is noteworthy that the soft X-ray selected sample does not contain extended soures (Paper I).

In this survey (i.e. in Paper I and this paper), we are dealing with the brightest previously unknown very soft RASS sources many of which turned out to be highly interesting individuals for which follow-up observations are warranted (see references given in the notes to Table 3).

2. Bright soft high galactic latitude sources

2.1. Sample definition

We consider an extension of the complete sample of bright high galactic latitude soft RASS X-ray sources studied in Paper I. That sample contained all RASS sources with total PSPC count rates[1] $CR \geq 0.5\,\mathrm{cts\,s^{-1}}$ and hardness ratios $HR1 < 0$ at galactic latitudes $|b| > 20°$. We intended the sample to be bounded by definite values of CR and $HR1$. Selection of the spectroscopic targets, however, was based on the very early analysis of the RASS (pre-RASS I, Voges et al. 1996) with count rates which were not based on the full information available in the RASS and which deviate, therefore, from the final ones of the RASS-II analysis. The latter entered the RASS Bright Source Catalogue (RASS BSC, Voges et al. 1999) and are used throughout this paper. As a consequence, the goal of a count rate limited sample could be met for the brighter sources of Paper I, but not

Send offprint requests to: beuermann@uni-sw.gwdg.de

* Based in part on observations with the ESO/MPI 2.2m telescope at La Silla, Chile

[1] The PSPC is the Position Sensitive Proportional Counter (Pfeffermann et al. 1986) onboard ROSAT, covering the photon energy range of 0.1–2.4 keV. The hardness ratio $HR1 = (H-S)/(H+S)$ with H and S the count rates in the hard and soft energy intervals of 0.5–2.0 keV and 0.1–0.4 keV, respectively.

for the fainter sub-sample presented here. The actual limiting factor was the available telescope time. The sources identified here have total PSPC count rates $0.11 < CR < 0.50\,\mathrm{cts\,s^{-1}}$.

2.2. X-ray analysis

As described in Paper I, we retrieved small Photon Event Tables (PETs) from the RASS which cover 50×50 arcmin^2 around the respective source. The derived positions, count rates, and hardness ratios generally agree within errors with those quoted in the RASS BSC and the latter were adopted. Analysing the PETs allowed us to visually inspect the X-ray images for source confusion and structure of the background. Data analysis was as described in Paper I. All sources were found to be consistent with being pointlike.

Three very soft sources, two of which are highly time-variable, were included in the present sample although they are not contained in the BSC. They were clearly present in the individual strips of the early RASS analysis, however, subsequently confirmed as discrete sources by the PET analysis, and later identified as two mCVs and one probable WD. Since these sources are not confused or anomalous in any way except for the noted variability, it is unclear why they did not pass the criteria for inclusion in the BSC.

2.3. Optical counterparts

In a first step of the identification program, the source positions were cross-correlated with various catalogues, including, SIMBAD, the NASA/IPAC Extragalactic Database (NED), a collection of X-ray catalogues, the Catalogue of Quasars and Active Galactic Nuclei (7th Edition) (Veron-Cetty & Veron 1996), the Parkes catalogue of radio sources etc. If a plausible known counterpart existed within or very close to the 90% confidence error radius of the X-ray source, the source was considered identified. As in Paper I, the 90-% confidence error radius was derived from the 1-σ positional uncertainty Δp given in the RASS BSC as

$$r_{90} = 1.65\ \Delta p. \qquad (1)$$

As plausible counterparts of sources of intermediate hardness ratios we accepted AGN and bright stars, particularly of spectral type dM or dK. WDs and AM Herculis binaries are plausible counterparts for the very soft sources with HR1 near –1.

In a second step, we produced finding charts for all sources which do not coincide with an object of known nature within the 90% error circle of the X-ray source. As for Paper I, we used generally available material such as the Digitized Sky Survey (DSS) or the ROE and APM catalogues of optical objects which are based on scans of the ESO/SERC IIIa-J or the POSS-I red (E) and blue (O) plates, respectively.

In a third step, short-exposure CCD images and low-resolution spectra were taken of the candidate counterparts. The southern sources were observed with telescopes at La Silla, Chile, mostly with the ESO/MPI 2.2-m telescope in MPI time, the northern sources with a variety of telescopes at the Observatoire de Haute-Provence, France, the Calar Alto Observatory, Spain, and the McDonald Observatory, Texas, USA. The instrumentation was as described in Paper I. The observations were mostly performed in the years 1992 to 1994. In the La Silla and Calar Alto runs, the equipment used required a CCD image to be taken in order to position the source on the slit. In most cases, we took only short-exposure V-band images which resulted in a photometric accuracy not much better than the spectrophotometry. We estimate the accuracy of the quoted V-band magnitudes (Table 3) to be ~ 0.1–0.2 mag (see also Paper I).

For some sources, the planned spectroscopic observations could not be performed, but the source was nevertheless considered identified if independent information on the nature of the optical counterpart exists. E.g. an X-ray source coinciding with a galaxy with bright nucleus is quoted as an AGN, although of unknown type and redshift (see Notes to Table 3).

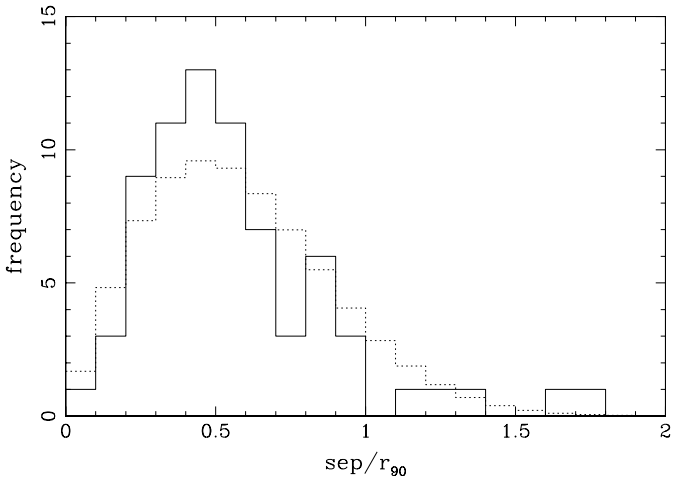

Fig. 1. Normalized separations between optical and X-ray positions in units of the 90%-confidence error radii as given by Eq. 1. The dashed histogram is the Gaussian. Two very soft sources have $sep/r_{90} > 2$ and are outside the panel.

3. Results

3.1. Unique counterparts

Fig. 1 shows the distribution of the normalized separations (in units of r_{90}) between the X-ray and optical positions of the spectroscopically identified counterparts in Table 3. Of 74 objects with measured separations, 67 or 93% have separations less than the 90 % confidence radius. A separation in excess of $3\,r_{90}$ is found only for one source, the very soft source RX J0515+01, a secure identification based on subsequent pointed ROSAT observations (Shafter et al. 1995). This is not surprising as it is known that the position uncertainties are largest for the softest sources (Voges et al. 1999). The agreement between the observed and expected distributions in Fig. 1 leads us to conclude that, for the large majority of the sources, a unique optical counterpart is present.

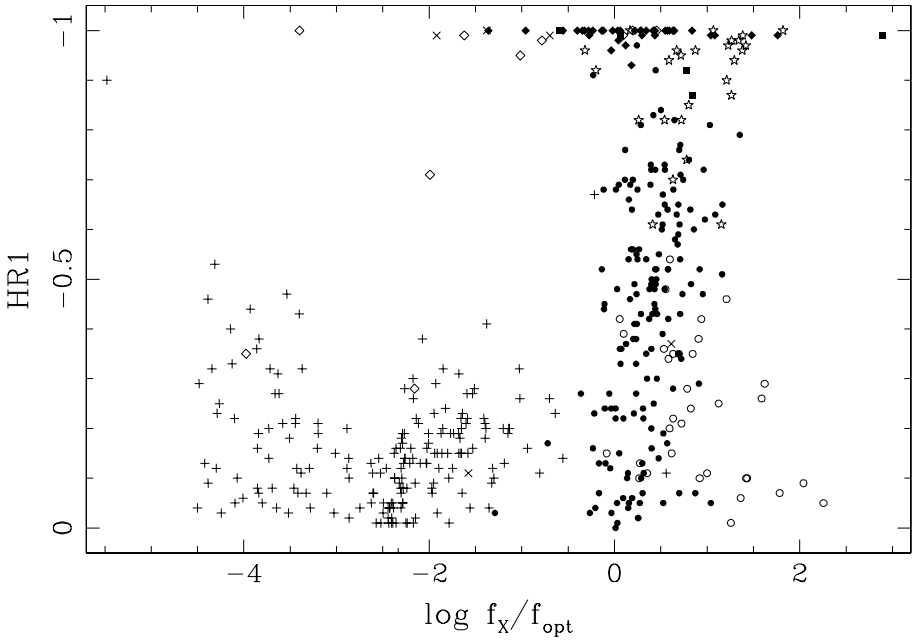

Fig. 2. Distribution of soft X-ray selected high galactic latitude RASS sources in the hardness ratio $HR1$ vs. $f_{\rm x}/f_{\rm o}$ plane (see text for an explanation of the abszissa). Sources shown are from Paper I and from this work. The symbols refer to stars (+), Sy1 galaxies and quasars (•), BL Lac objects (○), mCVs (asterisks), WDs (filled ⋄), WDs in binaries (open ⋄), supersoft sources (filled squares), other (×).

Table 1. Numbers of identified sources in different sub-classes of the present sub-sample of the soft high galactic latitude RASS sources (compare Paper I). Spectr. = spectroscopic identifications; Other = Identifications inferred by other means (see Notes to Table 3).

Class	Spectr.	Other
Coronal emitters	9	0
White dwarfs, PNN	8	1
Star+WD companion	0	0
CVs	10	0
AGN (Sy1, QSO)	43	4
AGN (BL Lac)	0	0
Total	70	5

Table 2. Number of objects for the individual subgroups of X-ray sources in the combined sample of Paper I and this paper, mean values of $\log(f_{\rm x}/f_{\rm o})$, and full range of $\log(f_{\rm x}/f_{\rm o})$.

Spectra type	number	$\log(\langle f_{\rm x}/f_{\rm o}\rangle)$	full range	
M star	53	–1.6	–2.4	–0.6
K star	54	–2.2	–4.0	–0.2
G star	49	–2.9	–3.9	–2.0
F star	29	–3.8	–4.5	–2.4
B/A star	4	–4.5	–5.5	–3.8
WD	38	0.2	–1.4	1.8
WD+star	10	–1.4	–4.0	0.5
mCV	27	0.8	–0.3	1.8
SSS	5	0.8	–0.6	2.9
AGN (Sy1, QSO)	158	0.4	–1.3	1.4
AGN (BL Lac)	34	0.9	–0.1	2.3

3.2. Source content

The source content of the present sub-sample is summarized in Table 1. As in Paper I, the number of newly identified coronal emitters is small because most stars detected in the RASS are sufficiently bright to have been previously catalogued. Such stars were excluded from the present identification program, although follow-up studies may be required to determine their detailed properties. AGN are by far the most frequent counterparts to the newly identified soft sources. With the exception of a few objects for which the relevant information is missing, all newly identified AGN are of spectral type Sy1. The occurrence of AGN with hardness ratios HR1 close to –1 demonstrates that Seyfert nuclei can have X-ray spectra which are almost as soft as those of thermal emitters like hot WDs. A particularly noteworthy example of this source type is the highly X-ray variable Seyfert galaxy WPVS007 (Paper I, Grupe et al. 1995). The properties of most soft X-ray selected AGN identified in Paper I and here are described by Grupe et al. (1998,1999).

Magnetic CVs represent another source class contributing to the present sample of soft X-ray sources. Of the 10 newly discovered CVs in this sample, 8 are Polars (or AM Herculis binaries) and 2 soft Intermediate Polars, a small sub-class first recognized with ROSAT (Haberl & Motch 1995, Burwitz et al. 1996). No non-magnetic CVs (disk accretors) were found among the soft high galactic latitude RASS sources (including those of Paper I), but several were identified in the Galactic Plane Survey (Motch et al. 1996a,b). Although many non-magnetic CVs are intrinsically faint X-ray sources (van Teeseling et al. 1996), they have harder spectra than the mCVs and can be detected at distances in the galactic plane larger than the scale height of the stellar disk.

The results on the identified sources demonstrate that the combined optical and X-ray properties can provide a first clue also on the nature of counterparts to X-ray sources which are not yet spectroscopically identified. Fig. 2 shows all newly identified sources reported in Paper I and in this paper in the $HR1$ vs. $f_{\rm x}/f_{\rm o}$ plane, where

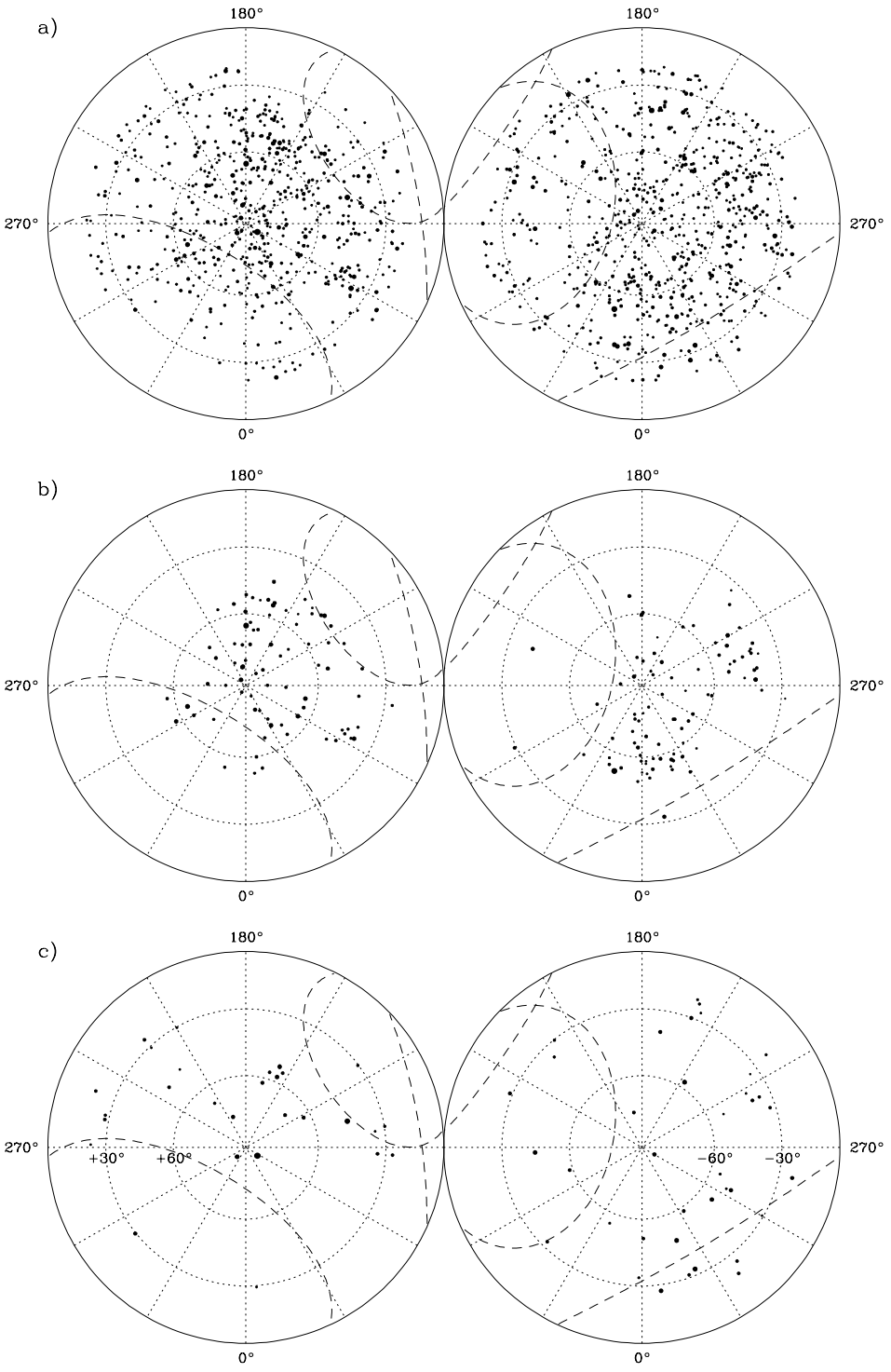

Fig. 3a–c. Distribution of soft bright high galactic latitude RASS sources over the sky. Both galactic hemispheres are shown down to the galactic equator with the selected sources plotted for galactic latitudes $\mid b \mid > 20^\circ$, leaving out the very densely populated galactic plane. The northern galactic sky is shown on the left, the southern on the right. The diameter of the dots is proportional to the logarithm of the total PSPC count rate CR. Dashed curves schematically indicate the galactic radio Loops I, II, and III (see text). *Upper panel:* All soft RASS sources with total PSPC count rates CR $> 0.2\,\mathrm{cts\,s^{-1}}$and hardness ratios $HR1 < 0$. *Center panel:* The AGN listed in Paper I and those newly identified in this paper. *Lower panel:* The newly identified very soft galactic X-ray sources (cataclysmic variables and white dwarfs) from Paper I and this paper.

$$\log(f_\mathrm{x}/f_\mathrm{o}) = \log CR + 0.4\,V - 5.86. \qquad (2)$$

We obtained this relation by converting the observed total PSPC count rate CR in $\mathrm{cts\,s^{-1}}$ into an energy flux using $f_\mathrm{x} = CR/ECF$ with the same energy conversion factor $ECF = 1.7 \times 10^{11}\,\mathrm{cts\,cm^2\,erg^{-1}}$ as taken by Zickgraf et al. (1997), and by converting the visual magnitude V into the integrated flux in the visual passband using $\log f_\mathrm{o} = -0.4\,V - 5.37$ (Maccacaro et al. 1988). Note that Fig. 2 includes the sources identified by us spectroscopically and those identified by cross-correlation with catalogues (which refers mostly to the coronal emitters). AGN of Seyfert type are found to populate a comparatively narrow strip with $f_\mathrm{x}/f_\mathrm{o} \simeq$ 1–100. The slight slant of this locus arises from the increased galactic absorption suffered on the average by the harder sources. The softest AGN reach into the regime of mCVs and WDs. AGN of BL Lac type have larger $f_\mathrm{x}/f_\mathrm{o}$ and $HR1 \gtrsim -0.5$. Stars (coronal emitters) typi-

cally have $HR1 \gtrsim -0.5$, too, but low $f_{\rm x}/f_{\rm o}$, with mean values of $\log\langle f_{\rm x}/f_{\rm o}\rangle$ ranging from –1 for M-stars to –4 for A/B stars. Table 2 lists the mean values and the ranges of $\log(f_{\rm x}/f_{\rm o})$. There seems to be a dichotomy in $\log(f_{\rm x}/f_{\rm o})$ for the coronal emitters with K/M stars and G/F stars clustering around $f_{\rm x}/f_{\rm o}\simeq -1.7$ and $f_{\rm x}/f_{\rm o}\simeq -3$, respectively. With this information, Fig. 2 may aid in predicting the nature of so far unidentified X-ray sources.

We have used, but not depicted here, variability between the numerous short sightings during the RASS as an additional parameter in the process of source identification. AGN, WDs, and mCVs blend in the upper part of Fig. 2. This degeneracy is lifted if variability is considered. Most mCVs display a large variability, AGN a less pronounced, and WDs no variability.

A complete list of the RASS sources identified in this paper is given in Table 3. The structure of the table is the same as that of Table 3 of Paper I and is explained there. The V-magnitudes in column 11 are either from the CCD images or from the flux-calibrated spectra. Column 12 refers to the notes given on indvidual sources.

3.3. Distribution over the sky

Fig. 3 shows the distribution of the soft RASS sources in both galactic hemispheres. Panel (a) contains all sources with negative $HR1$ down to $0.2\,{\rm cts\,s^{-1}}$(our approximate sensitivity limit), panel (b) the AGN listed in Paper I and those newly identified in this paper, and panel (c) the newly identified mCVs and WDs. Since the RASS sources were selected for negative hardness ratio, they are expected to cluster in regions of the sky with low column density of galactic neutral atomic hydrogen. Some major structures of the interstellar gas at galactic latitudes $|\,b\,| > 20^\circ$ are associated with the Galactic Radio Loops I, II, and III identified in the nonthermal radio continuum. We have schematically indicated these large-scale structures in Fig. 3 as dashed lines. The surface density of all soft RASS sources with PSPC count rate $> 0.2\,{\rm cts\,s^{-1}}$shows no strong dependence on galactic latitude, because the opposite latitude dependencies of galactic and of extragalactic sources approximately cancel. In particular, the surface density of coronal emitters (not separately shown) increases as the galactic latitude decreases. The surface density of soft X-ray selected AGN, on the other hand, is found to decrease drastically inside the Galactic Loops and generally at latitudes $|\,b\,| \lesssim 40^\circ$. WDs and mCVs follow the same pattern, although less pronounced, because some nearby objects are located in front of the absorbing gas. A clustering of the very soft X-ray selected stellar population was also noted by Warwick et al. (1993) and Diamond et al. (1995) for All-Sky Survey sources detected with the Wide Field Camera onboard ROSAT. The distribution over the sky of the sources discovered with the X-ray telescope onboard ROSAT provides additional information on the structure of local interstellar space (Thomas & Beuermann 1997).

Fig. 3 shows that the detection probability of soft X-ray emitting AGN, mCVs, and WDs varies substantially over the sky. Deriving the corresponding luminosity functions and/or space densities requires careful consideration of this probability as a function of position in the sky.

4. Conclusion

This program concludes our effort to identify the brightest soft X-ray sources from the ROSAT All-Sky Survey. Compared to the bulk of the unidentified sources, the 205 objects identified in Paper I and here represent the tip of the iceberg, only. The importance of the program lies in the fact that it provides identifications of individual sources which are sufficiently bright for detailed follow-up studies. At the same time, the present program has added to our knowledge of issues so diverse as the nature of soft X-ray emitting AGN, the properties of magnetic CVs, and the occurrence of supersoft X-ray sources. Further studies of individual sources are in preparation (see the notes to Table 3).

Acknowledgements. The ROSAT project is supported by the Bundesministerium für Bildung und Forschung (BMBF/DLR) and the Max-Planck-Gesellschaft. We thank the ROSAT team for performing the All-Sky Survey and producing the RASS Bright Source Catalogue. We also thank Drs. Frederic Hessman and Dirk Grupe for contributing part of the spectroscopic material and the referee Dr. Belinda Wilkes for helpful comments. This research has made use of the SIMBAD database operated at CDS, Strasbourg, France, and the NASA/IPAC Extragalactic Database (NED) operated by the Jet Propulsion Laboratory, California Institute of Technology under contract with the National Aeronautics and Space Asministration. Identification of the RASS X-ray sources was greatly facilitated by use of the finding charts based upon the COSMOS scans of the ESO/SERC J plates performed at the Royal Observatory Edinburgh and the APM catalogue based on scans of the red and blue POSS plates performed at the Institute of Astronomy, Cambridge, UK. This work has been supported in part by the BMBF/DLR under grants 50 OR 9210 1 and 50 OR 9403 5.

References

Bade N., Engels D., Voges W., et al., 1997, A&AS 127, 145
Beuermann K., Burwitz V., 1995, ASP Conf. Ser. 85, 99
Beuermann K., Thomas H.-C., 1993, Adv. Space Res. 13 (12), 115
Burwitz V., Reinsch K., Beuermann K., Thomas H.C., 1996, A&A 310, L25
Burwitz V., Reinsch K., Beuermann K., Thomas H.C., 1997, A&A 327, 183
Burwitz V., Reinsch K., Beuermann K., Thomas H.-C., 1999, Annapolis Workshop on Magnetic Cataclysic Variables, ASP Conf. Ser. 157, 127
Diamond C.J., Jewell S.J., Ponman T.J., 1995, MNRAS 274, 589
Grupe D., Beuermann K., Mannheim K., et al., 1995, A&A 300, L21
Grupe D., Beuermann K., Thomas H.-C., Mannheim K., Fink H.H., 1998, A&A 330, 25
Grupe D., Beuermann K., Mannheim K., Thomas H.-C., 1999, A&A in press
Haberl F., Motch C., 1995, A&A 297, L37
Hasinger G., 1994, Rev. Mod. Astr. 7, 129
Maccacaro T., Gioia I., Wolter A., Zamorani G., Stocke J.T., 1988, ApJ 326, 680
Mason K.O., Hassall B.J.M., Bromage G.E., et al., 1995, MNRAS 274, 1194

Table 3. Summary of optical identification program of new bright soft high-galactic-latitude RASS sources with HR1 < 0. Columns denote (1) the J 2000 X-ray position from the RASS BSC, (2) and (3) the J 2000 RA and DEC of the optical counterpart, (4) the separation between optical and X-ray positions in arcsec and (5) in units of the 90% confidence radii according to Eq. 1, (6) the RASS BSC PSPC count rate CR in $\mathrm{cts\,s^{-1}}$, (7) the hardness ratio HR1, (8) the class and (9) the type of the optical counterpart, (10) the redshift z if extragalactic, and (11) the visual magnitude V. Errors to CR and HR1 are given in brackets and refer to the last digits. Notes at the end of the table refer to the 1RXS J numbers in column (1).

(1) RASS BSC No. 1RXS J.....	(2) (3) RA,DEC(2000)	(4) (5) Separation ($''$) r_{90}	(6) CR	(7) HR1	(8) Class	(9) Type	(10) z	(11) V	(12) Notes
000647.2–332316	0 6 46.7 –33 23 11	8.0 0.35	0.141 (25)	–0.69 (11)	AGN	Sy1	0.217	16.9	1
002233.8–340722	0 22 33.2 –34 7 20	7.7 0.59	0.418 (37)	–0.38 (08)	AGN	Sy1	0.219	16.1	1,4,6
005033.3+244901	0 50 33.0 24 49 2	4.2 0.28	0.444 (58)	–0.20 (12)	STAR	dMe		12.6	1,3
012237.4–264646	1 22 37.4 –26 46 46	0.0 0.00	0.321 (42)	–0.65 (08)	AGN	Sy1	0.417	18.8	1,6
012326.1–794139	1 23 16.5 –79 41 33	26.5 1.79	0.282 (45)	0.05 (15)	STAR	K		10.2	1
013242.8–655434	1 32 42.0 –65 54 34	4.9 0.30	0.276 (38)	–0.97 (04)	CV	AM		20.0	1,8
013417.2–425821	1 34 16.8 –42 58 26	6.7 0.41	0.168 (23)	–0.91 (05)	AGN	Sy1	0.237	16.0	1,4
013653.5–351012	1 36 54.3 –35 9 53	21.4 1.63	0.491 (38)	–0.81 (04)	AGN	Sy1	0.289	18.0	1,4
	1 54 0.9 –59 47 49	21.9 1.11	0.335 (54)	–0.70 (07)	CV	AM		17.0	1,8
020403.1–510455	2 4 2.7 –51 4 57	4.3 0.33	0.439 (38)	–0.25 (08)	AGN	Sy1	0.151	16.6	1,4
021257.7–585109	2 12 58.1 –58 51 17	8.6 0.52	0.185 (53)	–0.10 (27)	STAR	dMe		13.7	1
021754.1–195813	2 17 53.6 –19 58 19	9.3 0.43	0.144 (24)	–0.37 (15)	AGN	Sy1	0.468	17.1	1,6
022815.6–405712	2 28 15.2 –40 57 16	6.0 0.46	0.437 (55)	–0.52 (10)	AGN	Sy1	0.494	15.2	1,4
024513.8–434410	2 45 14.1 –43 44 1	9.6 0.58	0.233 (36)	–0.41 (12)	STAR	dMe		13.8	1
030313.9–474214	3 3 14.2 –47 42 13	3.2 0.24	0.196 (23)	–0.30 (10)	AGN			17.3	5,8
031713.9–853231	3 17 20.0 –85 32 29	7.4 0.50	0.204 (22)	–1.00 (01)	STAR	WD		13.9	1,2
033550.1–471556	3 35 49.7 –47 16 0	5.7 0.39	0.245 (24)	–0.30 (09)	AGN	Sy1	0.598	17.3	1
033714.6–415541	3 37 15.1 –41 55 25	16.9 0.68	0.145 (34)	–1.00 (14)	STAR	WD		16.4	1
035514.0–545159	3 55 13.3 –54 51 57	6.4 0.43	0.216 (21)	–0.68 (07)	AGN	Sy1	0.269	16	1
043513.8–461524	4 35 14.3 –46 15 34	11.3 0.86	0.249 (38)	–0.48 (11)	AGN	Sy1	0.070	17.1	1,4
043554.2–363635	4 35 53.9 –36 36 42	7.9 0.60	0.445 (40)	–0.28 (08)	AGN	Sy1	0.141	17.1	1,4,7
043830.0–614758	4 38 29.3 –61 47 59	5.1 0.31	0.390 (68)	–0.00 (17)	AGN	Sy1	0.069	15.7	1,4
043943.2–454039	4 39 44.7 –45 40 43	16.2 0.90	0.319 (39)	–0.81 (07)	AGN	Sy1	0.224	16.6	1,4
044550.1–385537	4 45 50.7 –38 55 38	7.1 0.39	0.223 (36)	–0.97 (09)	STAR	WD		17.5	1
045223.8–164926	4 52 24.3 –16 49 18	10.7 0.72	0.431 (35)	–0.22 (07)	STAR	dMe		12.5	1
045444.5–481300	4 54 42.9 –48 13 19	24.8 0.84	0.145 (26)	–0.72 (11)	AGN	Sy1	0.363	17.7	1,4
045929.4–222953	4 59 28.9 –22 29 55	7.2 0.36	0.115 (19)	–0.83 (08)	GAL		0.047	18	1,8
050146.2–035927	5 1 46.1 – 3 59 32	5.2 0.29	0.224 (26)	–0.96 (03)	CV	AM		17.5	1,8
051214.5–324140	5 12 13.1 –32 41 38	17.8 1.35	0.151 (20)	–0.51 (10)	CV	IP		17.6	1,8
051541.7+010528	5 15 41.3 1 4 40	48.4 3.68	0.381 (32)	–0.92 (03)	CV	AM		15.5	1,8
054747.2–195609	5 47 46.9 –19 56 9	4.2 0.28	0.168 (21)	–0.92 (05)	AGN		0.055:	17.7	1,5,8
060033.1–270918	6 0 33.2 –27 9 19	1.7 0.13	0.404 (42)	–0.87 (04)	CV	AM		19	1,8
060452.1–343331	6 4 52.0 –34 33 43	12.1 0.92	0.428 (50)	0.06 (11)	STAR	dMe		13.4	1,2
061544.4–653151	6 15 43.6 –65 31 52	5.1 0.44	0.093 (05)	–0.03 (05)	AGN	Sy1	0.227	16.6	1
	8 6 21.7 15 27 15	7.3 0.40	0.158 (27)	–0.67 (10)	CV	IP		20	1,8
	8 36 50.3 15 53 28	35.8 2.71	0.246 (50)	–0.99 (01)	STAR	WD			1,8
085909.5+053703	8 59 9.2 5 36 55	9.2 0.51	0.233 (28)	–0.82 (06)	CV	AM		17	1,8
094538.0–005829	9 45 37.9 – 0 58 29	1.5 0.11	0.381 (31)	–0.15 (07)	STAR	K		11	1
095308.6+145841	9 53 8.1 14 58 37	8.3 0.50	0.185 (27)	–0.74 (08)	CV	AM		17.3	1,8
101402.5+461954	10 14 1.9 46 19 54	6.2 0.42	0.150 (19)	–0.66 (09)	AGN	Sy1	0.324	17.1	1,3,4,7
101718.0+291439	10 17 18.3 29 14 34	6.4 0.56	0.386 (34)	–0.24 (08)	AGN	Sy1	0.049	15.7	1,4,8
102444.5–302102	10 24 44.2 –30 20 59	4.9 0.30	0.201 (28)	–1.00 (03)	STAR	WD		15.8	1,2
104614.2+525600	10 46 13.7 52 55 54	7.5 0.57	0.322 (27)	–0.82 (04)	AGN	Sy1:	0.51:	17.5	1,3,8
105055.2+552731	10 50 55.2 55 27 23	8.0 0.69	0.374 (29)	–0.69 (05)	AGN	Sy1	0.333	16.7	1,3,4
105355.0+661209	10 53 55.6 66 12 1	8.8 0.67	0.179 (19)	–0.76 (06)	AGN	Sy1	0.117	16.8	1,3
105444.4+483145	10 54 44.7 48 31 38	7.6 0.66	0.454 (32)	–0.36 (06)	AGN	Sy1	0.286	15.7	1,3,7
110842.1+595010	11 8 41.6 59 50 8	4.3 0.33	0.160 (19)	–0.72 (07)	AGN	Sy1	0.425:	18	1,3,8
114738.0+050119	11 47 37.6 5 1 10	10.8 0.82	0.392 (33)	–0.13 (08)	STAR	dMe		12.1	1,3
120656.2+700754	12 6 55.2 70 7 49	7.1 0.62	0.436 (26)	–0.15 (05)	STAR	dMe		11.4	1,3
123220.6+495731	12 32 20.1 49 57 22	10.2 0.78	0.341 (31)	–0.60 (07)	AGN	Sy1	0.262	17	1,3

Table 3. (continued)

(1) RASS BSC No. 1RXS J.....	(2) (3) RA,DEC(2000)	(4) Separation ($''$)	(5) r_{90}	(6) CR	(7) HR1	(8) Class	(9) Type	(10) z	(11) V	(12) Notes
131259.1+262825	13 12 59.5 26 28 24	5.5	0.37	0.418 (39)	–0.41 (07)	AGN	Sy1	0.061	16	1,3,4,7
150204.3+064521	15 2 4.1 6 45 15	6.7	0.51	0.472 (50)	–0.52 (09)	AGN	Sy1	0.286	16.6	1,3
161418.7–083335	16 14 19.0 – 8 33 25	10.9	0.74	0.240 (26)	–1.00 (02)	STAR	WD		14	1
164625.8+392922	16 46 26.0 39 29 33	11.2	0.85	0.396 (28)	–0.42 (06)	AGN	Sy1	0.100	17.1	1,3,4
165240.0+441632	16 52 40.1 44 16 37	5.1	0.44	0.489 (29)	–0.56 (04)	AGN	Sy1	0.132	16.9	1,3,7
171127.2+664532	17 11 27.3 66 45 29	3.1	0.27	0.235 (10)	–1.00 (00)	STAR	WD		17	1,2
181810.0+534343				0.479 (18)	–0.35 (03)				15	8
202237.8–395412	20 22 37.3 –39 54 13	5.8	0.35	0.330 (36)	–0.97 (03)	CV	AM		18.5	1,8
203626.2–535222				0.144 (28)	–1.00 (05)	STAR	WD:			5,8
214406.1–394900	21 44 5.9 –39 49 2	3.1	0.24	0.412 (37)	–0.47 (07)	AGN	Sy1	0.140	18.0	1,4
215450.7–441406	21 54 51.0 –44 14 6	3.2	0.24	0.454 (39)	–0.70 (06)	AGN	Sy1	0.344	15.8	1,4
220416.7–425817	22 4 17.5 –42 58 14	9.3	0.40	0.217 (30)	–0.72 (09)	AGN	Sy1	0.639	18.7	1
220546.4–405816	22 5 45.4 –40 58 18	11.5	0.64	0.154 (25)	–0.68 (10)	AGN	Sy1	0.235	18.3	1
221300.5–171015	22 13 0.1 –17 10 19	7.0	0.53	0.425 (42)	–0.58 (07)	AGN	Sy1	0.146	17.2	1,4,6
221515.2–274225	22 15 14.7 –27 42 22	7.3	0.40	0.315 (39)	–1.00 (02)	STAR	WD		15.5	1
222149.3–271310	22 21 48.4 –27 13 13	12.4	0.94	0.287 (34)	–0.57 (08)	AGN	Sy1	0.177	17.7	1,4,7
222650.8–414442	22 26 50.6 –41 44 46	4.6	0.31	0.169 (27)	–0.69 (10)	AGN	Sy1	0.307	17.0	1,7
223003.8–513702	22 30 4.1 –51 37 7	5.7	0.39	0.217 (27)	–0.51 (10)	AGN	Sy1	0.454	19.2	1
223244.3–413441	22 32 43.0 –41 34 38	14.9	0.91	0.190 (28)	–0.56 (12)	AGN	Sy1	0.075	16.9	1,4,7
224155.3–440459	22 41 55.3 –44 4 55	4.0	0.27	0.359 (39)	–0.68 (07)	AGN	Sy1	0.545	15.8	1,4
224642.0–520638	22 46 42.1 –52 6 40	2.2	0.17	0.706 (67)	0.14 (09)	GAL		0.194	18.2	1,8
230358.7–551717	23 3 57.8 –55 17 18	7.8	0.59	0.375 (34)	–0.34 (08)	AGN	Sy1	0.084	17.5	1,4
230439.3–512804	23 4 38.4 –51 28 0	9.3	0.63	0.356 (39)	–0.52 (09)	AGN	Sy1	0.106	17.2	1,4
233711.4–593241	23 37 9.0 –59 32 25	24.3	1.23	0.163 (30)	–0.56 (14)	AGN	Sy1	0.567	17.3	1
234024.3–532913	23 40 23.0 –53 28 57	19.8	0.86	0.230 (46)	–0.73 (14)	AGN	Sy1	0.321	17.6	1,4
234907.7–331148	23 49 7.3 –33 11 44	6.4	0.49	0.458 (46)	–0.49 (08)	AGN	Sy1	0.144	16.6	1,4,6,7
234939.7–563723				0.490 (62)	–0.79 (07)					8

1: Spectroscopic identification, this work
2: WFC identification (Pye et al. 1995, Mason et al. 1995)
3: Hamburg/RASS identification (Bade et al. 1997)
4: see also Grupe et al. 1998
5: Inferred identification from the Digitized Sky Survey
6: Radio source
7: Listed also by Veron-Cetty & Veron (1996)
8: Remarks to individual sources

013242.8–655434: AM Herculis binary (Burwitz et al. 1996)
015400.9–594749: AM Herculis binary (Beuermann & Thomas 1993). The variable X-ray source is not contained in the RASS BSC. The J 2000 X-ray position derived from the PET is 1 54 00.8 –59 48 10.
030313.9–474214: CCD image shows galaxy with bright nucleus within $3''$ from X-ray position, B = 18.2 (ROE finding chart). The 14 mag star $20''$ NE of spectral type ∼K1 is probably unrelated to the X-ray source
045929.4-222953: Our R filter image shows a galaxy with a bright core. Our two spectra show red-shifted absorption lines of the galaxy but no emission lines.
050146.1–035932: AM Herculis binary (Burwitz et al. 1999)
051213.1–324138: Soft Intermediate Polar (Burwitz et al. 1997)
051541.3–010440: AM Herculis binary (Shafter et al. 1995)
054747.2-195609: The CCD image shows galaxy with bright nucleus $5''$ W of X-ray position. Our spectrum misses the nucleus and shows a weak absorption spectrum with z = 0.055:. A probably unrelated late F star is $31''$ E
060033.2–270919: AM Herculis binary (Beuermann & Burwitz 1995)
080621.7–152715: Intermediate Polar. The highly variable X-ray source is not contained in the RASS BSC. The J 2000 X-ray position derived from the PET is 8 06 22.2 15 27 14
083650.3–155328: White dwarf. Only a non-calibrated spectrum is available. The X-ray source is not contained in the RASS BSC. The J 2000 X-ray position derived from the PET is. 8 36 52.2 15 53 51
085909.5–053703: AM Herculis binary (Beuermann & Burwitz 1995), V = 16.5–18.7
095308.1–145837: AM Herculis binary (Beuermann & Burwitz 1995)

Table 3. (continued)

101718.0+291439: This active galaxy is known as CASG 59 (Salzer et al. 1995)
104614.2+525600: The Hamburg survey lists this source as an AGN. Our segments of blue and red spectra miss MgII and Hβ. Hγ is very weak. Weaker spectral features yield $z = 0.510 \pm 0.003$.
110842.1+595010: Our spectrum contains only one Balmer line adjacent to a broad Fe-line complex. Interpreting the line as Hβ. yields the quoted redshift.
181810.0–534343: The 90% confidence error circle contains three objects. The $V \sim 15$ object 15″ SW is a G-star, no spectrum is available of the $V = 14.5$ candidate 5″ NE and the $V \sim 19$ candidate 12″ SSE.
202237.3–395413: AM Herculis binary (Burwitz et al. 1996)
203626.2–535222: HR1 $\simeq -1$ suggests a WD. Candidate 1 is $\sim 20''$ NW, has B = 12, and is of spectral type ∼K0; candidate 2 is 10″ E, has B = 17 and B–V = 0.6; candidate 3 is 23″ E, has B = 16 and B–V = 0.9. If the WD is associated with the K-star it should be fainter than $B \simeq 15.5$
224642.0–520638: Galaxy, no emission lines. Final $CR - HR1$ values place the source outside our sample.
234939.7–563723: A close pair of a B = 13 star of spectral type ∼K0 and an ∼15 mag object is 19″ NW, two faint red objects 18″ S. The X-ray source is variable and could be an AGN or a CV.

Correction to Paper I

160518.5+542101: For this source, the identification of Bade et al. (1997) as an M-star has been cited in Paper I. That star, however, is 31″ from the X-ray position and the more likely candidate is a 19 mag object at 5″ separation which is also a radio source (White et al. 1997), suggesting a BL Lac identification. For the M-star, the implied $f_{\rm x}/f_{\rm o} \simeq 0.44$ would also be quite atypical, while the $f_{\rm x}/f_{\rm o} \simeq 1.4$ is typical of a BL Lac object. The USNO-A1.0 optical position of the BL Lac candidate is RA, DEC (2000): 16 05 19.0, 54 21 00, the radio position RA, DEC (2000): 16 05 19.1, 54 21 00.

Motch C., Guillot P., Haberl F., et al., 1996a, A&A 318, 111
Motch C., Guillot P., Haberl F., et al., 1996b, A&AS 122, 201
Nugent J.J., Jensen K.A., Nousek J.A., et al., 1983, ApJS 51, 1
Pfeffermann E., Briel U.G., Hippmann H., et al., 1986, SPIE 733, 519
Pye J.P., McGale P.A., Allan D.J., et al., 1995, MNRAS 274, 1165
Salzer J.J., Moody J.W., Rosenberg J.L., et al., 1995, AJ 109, 2376
Shafter A.W., Reinsch K., Beuermann K., et al., 1995, ApJ 443, 319
Thomas H.-C., Beuermann K., 1997, Proc. of IAU Coll. 166, Springer LNP 506, 247
Thomas H.-C., Beuermann K., Reinsch K., et al., 1998, A&A 335, 467 (Paper I)
van Teeseling A., 1997, ASP Conf. Ser. 137, 385
van Teeseling A., Beuermann K., Verbunt F., 1996, A&A 315, 467
Veron-Cetty M.P., Veron P., 1996, ESO SR 17, 1
Voges W., 1997, The All-Sky Survey and Pointing Catalogues of ROSAT. in: Proceedings of the Fifth Workshop on "Data Analysis in Astronomy", Eds. V. Di Gesu, M.J.B. Duff, A. Heck, M.C. Maccarone, L. Scarsi, H.U. Zimmermann, World Scientific Publishing Co., Singapore, p. 189
Voges W., Boller T., Dennerl K., et al., 1996, In: Zimmermann H.U., Trümper J., Yorke H. (eds.) Proc. Röntgenstrahlung from the Universe. MPE Report 263, p. 637
Voges W., Aschenbach B., Boller Th., et al., 1999, A&AS in press
Warwick R.S., Barber C.R., Hodkin S.T., Pye J.P., 1993, MNRAS 262, 289
White R.L., Becker R.H., Helfand D.J., Gregg M.D., 1997, ApJ 475, 479
Zickgraf F.-J., Thiering I., Krautter J., et al., 1997, A&AS 123, 103